

## Kinetics of CuPt-type ordered phase formation in III-V semiconductor alloys during (001) epitaxial growth due to step flow

Manabu Ishimaru,\* Syo Matsumura,<sup>†</sup> Noriyuki Kuwano, and Kensuke Oki

*Department of Materials Science and Technology, Graduate School of Engineering Sciences, Kyushu University 39, Kasuga, Fukuoka 816, Japan*

(Received 26 August 1994)

In the present work, we carried out Monte Carlo simulations in order to investigate the effects of surface steps on CuPt-type ordering in III-V semiconductor alloys grown on a slightly inclined (001) substrate, on the basis of an Ising-like crystal growth model. Two types of surface steps were considered: one is the surface step along the  $[\bar{1}\bar{1}0]$  direction (the  $[\bar{1}\bar{1}0]$  step), and the other is the surface step along the  $[110]$  direction (the  $[110]$  step). The former and the latter have a preference for unlike- and like-atom pairs along the step edge, respectively. Flows of the  $[\bar{1}\bar{1}0]$  step leave CuPt-ordered domains of  $(\bar{1}\bar{1}1)$  and  $(\bar{1}\bar{1}\bar{1})$  variants with low degree of order. The domains elongate perpendicular to the growth direction of the crystal. After flows of the  $[110]$  step, on the other hand, only one variant is formed and large ordered domains grow from the interface with a substrate up to the top surface of the layer. The features of domain structure, such as the selection of variants and the morphology of the antiphase domains, are in good agreement with the previous experimental results obtained by transmission electron microscopy. It was found that (001) interplane interactions, which contribute to the ordering along the growth direction, play an important role for the difference of microstructures depending on the type of surface step. We also discuss the microstructure of the epilayer obtained by the motion of both surface steps on the surface layers.

### I. INTRODUCTION

A variety of techniques of epitaxial growth are currently employed to obtain high quality semiconductor films. In thin films of III-V semiconductor alloys grown by such techniques, some interesting phenomena which cannot be observed in bulk alloys have been reported. Although most bulk III-V semiconductor alloys ( $A_{1-x}B_x$ ) $C$  have a tendency toward phase separation in  $AC$  and  $BC$ , some ordered structures have been found in epilayers of the alloys grown by vapor phase epitaxy, such as molecular-beam epitaxy or organometallic vapor phase epitaxy.<sup>1-9</sup> Since the appearance of ordered phases influences material properties, such as the magnitude of band-gap energy<sup>7-9</sup> and electron mobility, it is important to make the mechanism of the ordering clear. Moreover, it is interesting that a CuPt-type ordered structure, which had been confirmed in only a few bulk systems,<sup>10,11</sup> has often been observed in many epitaxial layers. In the present work, we focus on the process of CuPt-type ordering in the epitaxial layers of III-V semiconductor alloys.

Srivastava, Martins, and Zunger<sup>12</sup> and Ferreira, Wei, and Zunger<sup>13</sup> carried out first-principles calculations to search for the most stable atomic configuration in III-V alloys and the equilibrium phase diagrams. They concluded that the bulk alloys have an equilibrium state of phase separation, and that the CuPt-type structure has the highest internal energy. On the other hand, it was experimentally confirmed that only  $(\bar{1}\bar{1}1)$  and  $(\bar{1}\bar{1}\bar{1})$  variants out of the four possible CuPt variants are formed in the epilayer.<sup>2</sup> These theoretical and experimental results indicate that the appearance of the ordered phase cannot be

explained as a bulk phenomenon, and Gomyo, Suzuki, and Iijima<sup>2</sup> have also discussed the importance of the surface during the crystal growth in their early manuscript. Note that the four equivalent  $\{111\}$  variants of CuPt structure in the bulk state divide into two classes in the presence of a surface:  $(111)$  and  $(1\bar{1}\bar{1})$ , called the CuPt<sub>A</sub> variant; and  $(\bar{1}\bar{1}1)$  and  $(\bar{1}\bar{1}\bar{1})$ , the CuPt<sub>B</sub> variant. Cao and co-workers<sup>14,15</sup> investigated the effect of growth rates on CuPt-type ordering in Ga<sub>1-x</sub>In<sub>x</sub>P, and showed that the high growth rates suppress the ordering. Their result suggests that the ordering requires diffusion of atoms on the top surfaces. Further, Gomyo, Suzuki, and Iijima<sup>2</sup> pointed out that the atomic steps on an inclined surface play an important role in the formation of the ordered structure. Transmission electron microscope (TEM) observations have revealed that the substrate orientation significantly affects CuPt-type ordering in Ga<sub>1-x</sub>In<sub>x</sub>P,<sup>2-4</sup> GaAs<sub>1-x</sub>P<sub>x</sub>,<sup>5</sup> and InAs<sub>1-x</sub>P<sub>x</sub> (Ref. 6) epilayers: when the (001) substrate is slightly inclined toward the  $[\bar{1}\bar{1}0]$  direction, the well-developed ordered domains, which consist of only one CuPt<sub>B</sub> variant out of the four possible CuPt variants, grow from the substrate into the surface layer. If the substrate is inclined toward the  $[110]$  direction, on the other hand,  $(\bar{1}\bar{1}1)$  and  $(\bar{1}\bar{1}\bar{1})$  variants with a low degree of order coexist, and the CuPt domains elongate perpendicular to the growth direction. A theory for the ordering mechanism which can explain these domain structures remains an open question.

Recently, we proposed an Ising-like model for the layer-by-layer growth of III-V semiconductor alloys, in which pairwise interactions between the first- and second-nearest-neighboring atoms were taken into ac-

count, and calculated the phase diagrams of the ground-state structures as a function of the interactions.<sup>16</sup> The result suggests that the CuPt-type ordered phase, which is unstable in bulk alloys, can be formed easily on the top surface layers during the growth. Using the model, we carried out a Monte Carlo simulation to investigate the CuPt ordering at finite temperatures.<sup>17</sup> Features of the Fourier power spectra of the atomic arrangements obtained by the simulation, such as the presence of wavy diffuse streaks and the dependence of the intensity maximum position in the streak upon the growth rate<sup>14</sup> and temperature,<sup>2</sup> were in complete agreement with those of transmission electron-diffraction patterns. These results all demonstrate that our model is quite useful for discussing the ordering mechanism and phase state in epitaxial layers.

In the present work, our growth model is applied to the surface-step-flow process to interpret a CuPt-type ordered microstructure in an epilayer grown on an off-angle substrate. The kinetics of the ordered phase formation is discussed in terms of the atomic pairwise interactions. We also present characteristics of the microstructures obtained by the Monte Carlo simulation and by TEM observation.

## II. MODEL AND SIMULATION METHODS

### A. Ising-like model for step-by-step growth

Figure 1 shows a (001) surface with an atomic step of an  $(A_{0.5}B_{0.5})^{\text{III}}C^{\text{V}}$  alloy with a zinc-blende structure. Open and closed circles denote atomic sites of III and V

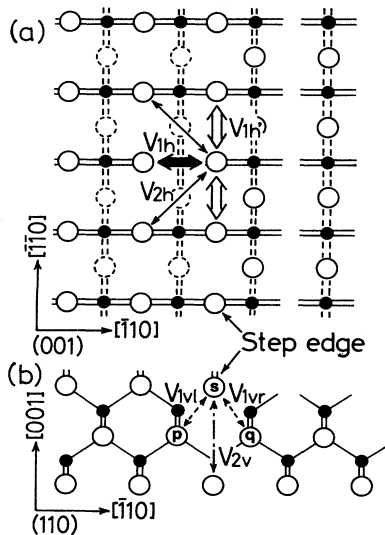


FIG. 1. Pairwise interactions between the first- and second-nearest-neighbor atoms in the fcc sublattice. (a) (001) and (b) (110) views. Open circles refer to group-III element sites in the top surface, and closed and dashed circles to group-V element sites in the underlying plane and group-III element sites in the next underlying plane, respectively. A surface step runs parallel to the [110] direction.  $s$ : atoms at the step edge.  $p$  and  $q$ : inter-layer first nearest partner atoms of  $s$  atoms.

elements, respectively. Atoms of  $A$  and  $B$  elements at the step edge [marked by  $s$  in Fig. 1(b)] are assumed to interact with their first- and second-neighbor atoms in the fcc sublattice, as indicated in Figs. 1(a) and 1(b). Here  $V$ 's are pairwise interaction parameters defined in the same way as in our previous work.<sup>17</sup> In this system, like-atom pairs are preferred when the parameter is positive, and unlike-atom pairs when it is negative. From an experimental observation for  $\text{Ga}_{1-x}\text{In}_x\text{P}$  alloys grown on (001) substrates,<sup>2,3</sup> it is found that unlike-atom pairs, i.e., Ga-In, are formed along the  $[1\bar{1}0]$  direction, and like-atom pairs, i.e., Ga-Ga or In-In, are arranged along the  $[110]$  direction. In the present work, therefore, we adopt  $V_{1h} < 0$  and  $V'_{1h} > 0$ , so that the  $[1\bar{1}0]$ - and  $[110]$ -step edges, respectively, have a tendency toward forming unlike- and like-atom pairs along the step edge. It should be noted that the value for  $V_{1v}$  of the  $s$ - $p$  atom pair is different from that of the  $s$ - $q$  pair, since the  $p$  atom is covered with an upper atomic layer of the III elements but the  $q$  atom is not. Hereafter, we designate the interactions as  $V_{1v1}$  and  $V_{1vr}$ , as shown in Fig. 1(b). Only the atoms at the step edge undergo rearrangements, following a standard Monte Carlo algorithm<sup>18</sup> of spin-flip dynamics. The configuration of atoms freezes after the next atomic line is deposited. The number of the sites of  $A$  or  $B$  atoms on a surface is  $64 \times 64$ , and the epitaxial layer is assumed to grow by repeating the above procedure.

We considered two types of straight surface steps, as shown in Fig. 2. One is the  $[110]$ -step flow to the  $[\bar{1}\bar{1}0]$  direction (the  $[110]$ -step flow), and the other is the  $[1\bar{1}0]$ -step flow to the  $[\bar{1}\bar{1}0]$  direction (the  $[1\bar{1}0]$ -step flow). The  $[110]$  and  $[1\bar{1}0]$  steps are introduced on the (001) substrate slightly inclined toward the  $[1\bar{1}0]$  and  $[\bar{1}\bar{1}0]$  directions, respectively. In our model, the anisotropy of

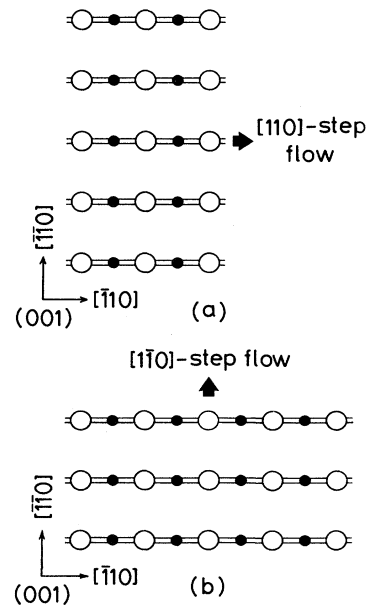


FIG. 2. Direction of surface step flows considered in this study. (a)  $[110]$  step moving in the  $[\bar{1}\bar{1}0]$  direction (the  $[110]$ -step flow). (b)  $[1\bar{1}0]$  step in the  $[\bar{1}\bar{1}0]$  direction (the  $[1\bar{1}0]$ -step flow).

the steps, e.g., the difference in flow-rate between the two step flows and the curvature of surface steps during the crystal growth,<sup>19</sup> is not taken into account.

### B. Treatment of surface-atom reconstruction

Surface-atom reconstruction is believed to have a large effect on ordering in III-V semiconductor alloys. Actually, Murgatroyd, Norman, and Booker<sup>20</sup> observed the existence of reconstruction on (001) surfaces in molecular-beam-epitaxy-grown  $\text{GaAs}_{1-x}\text{Sb}_x$  alloys, using *in situ* reflection high-energy electron diffraction. Some investigators<sup>3-5,20-22</sup> built models in which the role of surface reconstruction for CuPt-type ordering is taken into account. However, the ordering under consideration is substitutional ordering, and then the change in internal energy associated with an exchange of atomic species is essential. Therefore, the choice of atomic species to be paired is controlled by the energy change whether the surface is reconstructed or not. Insofar as a pairwise approximation is acceptable, our model is still valid for the case where the surface is reconstructed, provided that appropriate energy parameters are used. According to the first-principles calculation,<sup>23</sup> the absolute values of the pairwise interactions in the reconstructed structure are much larger than those in the unreconstructed one. The values used in our simulation were determined so that the ordering temperature would become comparable to the experimental one. Therefore, the present expression implicitly involves the effect of reconstruction. The interaction parameters used were  $V'_{1h} > 0$ ,  $V_{1h} = -0.8V'_{1h}$ ,  $V_{2h} = -0.5V'_{1h}$ , and  $V_{2v} = -0.3V'_{1h}$ . The growth temperature was  $T = V'_{1h}/k_B$ . The time interval was  $\Delta\tau = 20$  MCS (Monte Carlo step).

## III. RESULTS OF MONTE CARLO SIMULATIONS AND TEM OBSERVATIONS

### A. Crystal growth with the $[\bar{1}10]$ -step flow

As stated in Sec. II, the value of  $V_{1v1}$  is different from that of  $V_{1vr}$ . Our preliminary calculation confirmed that the asymmetry of interactions  $V_{1v}$  with respect to the position of the step edge,  $V_{1vr} - V_{1v1} = \Delta V_{1v}$ , determines which variant of the two  $\text{CuPt}_B$  types appears; in (110) Fourier transforms of the atomic arrangement obtained through the  $[\bar{1}10]$ -step flow, sharp superlattice spots of  $1/2\bar{1}/21/2$  type arise in the case when  $\Delta V_{1v} < 0$ , and those of  $\bar{1}/21/21/2$  type in the case when  $\Delta V_{1v} > 0$ . This indicates that only one variant of  $\text{CuPt}_B$  type is formed in the crystal grown by the  $[\bar{1}10]$ -step flow. According to previous experimental studies,<sup>2-4</sup> it has been found that the  $(\bar{1}11)$  variant appears when the  $[\bar{1}10]$  step flows to the  $[\bar{1}10]$  direction. This variant selection coincides with the case of  $\Delta V_{1v} > 0$ , showing that the absolute value of  $V_{1vr}$  should be larger than that of  $V_{1v1}$  in III-V semiconductor alloys.

Figure 3 shows a (110) projection of the atomic configuration for  $\Delta V_{1v} > 0$ . Here the open and closed circles denote *A* and *B* atoms, respectively. Semiclosed circles indicate that the atom columns contain *A* and *B*

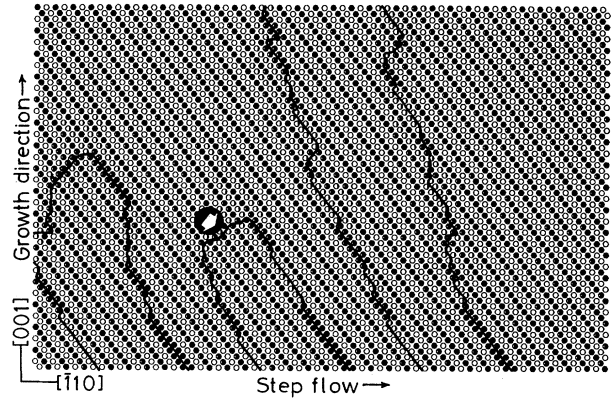


FIG. 3. A (110) projection of the atomic arrangement obtained by the  $[\bar{1}10]$ -step flow. Open, closed, and semiclosed circles denote that the atomic columns are *A* atom rich, *B* atom rich, and an equal mixture of *A* and *B* atoms, respectively. Solid lines indicate antiphase boundaries existing in the epilayer. The interaction parameters are  $V_{1vr} = 0.9V'_{1h}$  and  $V_{1v1} = 0.5V'_{1h}$  ( $\Delta V_{1v} = V_{1vr} - V_{1v1} > 0$ ).

atoms. In the present simulation, six antiphase boundaries (APB's) are inserted into the first layer on purpose, in order to investigate how the APB's develop during epitaxial growth. One can see that open- and closed-circle rows are alternately arranged along the  $[\bar{1}11]$  direction, showing that  $\text{CuPt}$  domains are well developed. APB's generated from the interface with the substrate develop upward. Most of them are of nonconservative type, and are almost parallel to the  $(\bar{1}11)$  planes, while the rest tend to be pulled in the direction of the step flow. An APB has a chance to encounter its adjacent APB and form a hairpin, as indicated by the arrow. Therefore, the density of APB's in the upper part of an epilayer is smaller than that near the interface with the substrate due to the self-annihilation process. The results obtained here excellently reproduce some features of the microstructure in actual III-V epilayers,<sup>3</sup> though we consider only pairwise interactions between first- and second-neighboring atoms. Thus our crystal-growth model includes an essential point for the ordering during the epitaxial growth.

### B. Crystal growth with the $[\bar{1}\bar{1}0]$ -step flow

Figure 4 shows a (110) Fourier power spectrum of the atomic arrangement obtained by the  $[\bar{1}\bar{1}0]$ -step flow. The parameters in the calculations were the same as in Fig. 3. There exist diffuse streaks passing through  $\bar{1}/21/21/2$ , and equivalent positions along the growth direction. It should be noted that in Fig. 4 the streaks curved toward the fundamental spots are wavy in shape. The wavy diffuse streaks are actually observed in the diffraction patterns for  $\text{Ga}_{1-x}\text{In}_x\text{P}$  grown on a (001) substrate inclined toward the  $[\bar{1}10]$  direction.<sup>3,14,15</sup> Intensity maxima exist in the streaks around  $\bar{1}/21/21/2$  and  $1/2\bar{1}/21/2$  positions, and the result suggests that  $(\bar{1}11)$  and  $(\bar{1}\bar{1}1)$  variants with low degrees of order coexist in

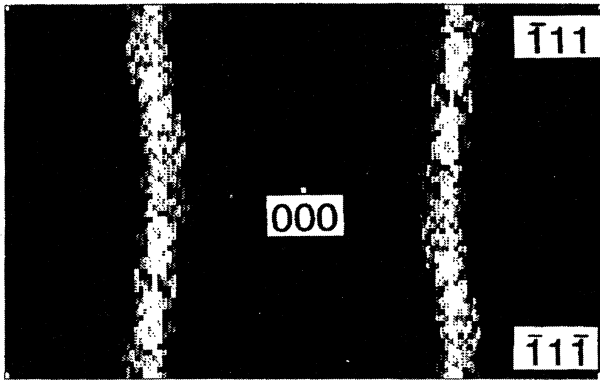


FIG. 4. A (110) Fourier power spectrum of atomic arrangement obtained by the  $[1\bar{1}0]$ -step flow. The interaction parameters are set to be the same as used in Fig. 3. Although the same parameters are used, no sharp superlattice spots appear in this spectrum, in contrast to the result of the  $[110]$ -step flow.

the epitaxial layer. It should be noted that the degree of CuPt ordering in the  $[1\bar{1}0]$ -step flow is much smaller than that in the  $[110]$ -step flow, although all the parameters, which include  $\Delta\tau$ , used in the simulations have the same values. The phenomenon can be explained as follows. In the  $[110]$ -step flow, the pairwise interactions, acting effectively upon ordering for the first-nearest neighbor between (001) interlayers, are proportional to  $(V_{1v} - V_{1v1})$ , and the asymmetric interactions introduce the alternate stacking of  $(\bar{1}11)$  pure elemental planes. In the  $[1\bar{1}0]$ -step flow, on the other hand, asymmetry makes no contribution to the CuPt ordering; there is no difference in the total of first-nearest-neighbor pairwise interactions, whether an *A* or *B* atom occupies a certain site of the step edge. The CuPt ordering along the growth direction is developed by the energy gain in the second-nearest-neighbor interaction  $V_{2v}$  only.

Figure 5 demonstrates a projection of the atomic arrangement from which the Fourier power spectrum of

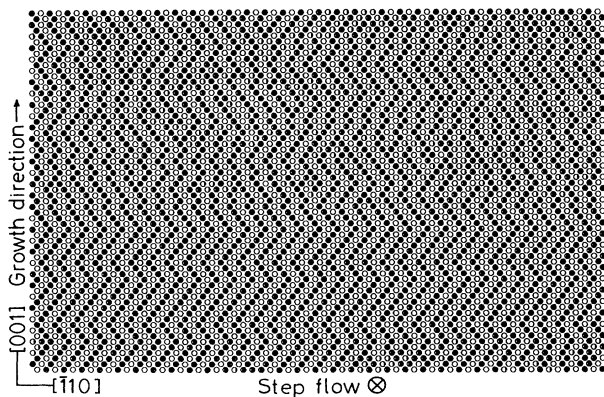


FIG. 5. A (110) projection of atomic arrangements corresponding to the Fourier spectrum of Fig. 4. There are many stacking faults, such as APB's and twin boundaries, in the epilayer. The platelike domains are best seen by viewing the page obliquely along the  $[\bar{1}11]$  or  $[1\bar{1}1]$  directions.

Fig. 4 was obtained. Ordered structures with a double periodicity along the  $[\bar{1}11]$  or  $[1\bar{1}1]$  direction are formed in the epitaxial layer, showing the appearance of two CuPt<sub>B</sub> variants. Platelike ordered domains are developed in Fig. 5, and the morphology of the microstructure is entirely different from that of Fig. 3. Many stacking faults, such as APB's in the ordered structure and twin boundaries between two variants, are inserted perpendicularly to the growth direction. The atomic column arrangement exhibits a zigzag pattern, and it is quite similar to a high-resolution TEM image of Ga<sub>1-x</sub>In<sub>x</sub>P reported by Baxter, Stobbs, and Wilkie.<sup>24</sup> According to diffraction theory, the existence of (001) plane faults and the plate-shaped ordered phases causes the streaks along the [001] direction. It is interesting that the shape of ordered domains and the amount of stacking faults depend sensitively on the step flow direction. Results, such as the existence of many stacking faults and the morphology of ordered domains, are in good agreement with those obtained experimentally for Ga<sub>1-x</sub>In<sub>x</sub>P grown on a (001) substrate with a misorientation in the  $[110]$  direction.<sup>3</sup>

### C. CuPt ordering in the case of the coexistence of the $[110]$ and $[1\bar{1}0]$ steps

From the results of Secs. III A and III B, we believe that when the  $[110]$  and  $[1\bar{1}0]$  steps move simultaneously in the  $[\bar{1}10]$  and  $[110]$  directions, respectively, two CuPt<sub>B</sub> variants may appear in the epitaxial layer. One can expect that the  $(\bar{1}11)$  variant consists of coarse and fine domains and the  $(1\bar{1}1)$  variant fine domains only, because the  $[110]$ -step flow which produces the coarse domains makes no contribution to the formation of the latter variant. In order to confirm the expectation, we have examined the microstructures of a Ga<sub>1-x</sub>In<sub>x</sub>P alloy grown on a (001) GaAs substrate inclined in the  $[011]$  direction by means of TEM.

Figure 6 shows an electron-diffraction pattern of the specimen. The electron incidences of Figs. 6(a) and 6(b) are parallel to the  $[110]$  and  $[1\bar{1}0]$  directions, respectively. In the (110) pattern, reflections at 001 and the equivalent positions occur by double diffraction. Superlattice spots arise at  $\bar{1}/2\ 1/2\ 1/2$  and  $1/2\ \bar{1}/2\ 1/2$  positions, but they do not in the  $(1\bar{1}0)$  pattern, indicating that two ordered variants are formed in this epilayer. We should notice that the  $\bar{1}/2\ 1/2\ 1/2$  reflection is stronger than the  $1/2\ \bar{1}/2\ 1/2$  one in the diffraction pattern. The asymmetry suggests that in the crystal the  $(\bar{1}11)$  domains are large in quantity and have a high degree of order compared with the  $(1\bar{1}1)$  ones. The best account for the phenomenon can be found in the number of surface steps which contribute to the formation of each variant. That is, the  $(\bar{1}11)$  domains are produced by both of the  $[110]$ - and  $[1\bar{1}0]$ -step flows, but the  $(1\bar{1}1)$  domains can be formed only by the  $[1\bar{1}0]$ -step flow. The strong effects of surface steps on the superstructure intensity asymmetry is also pointed out by Gomyo, Suzuki, and Iijima.<sup>2</sup> In addition to these reflections, diffuse scatterings connecting the superlattice spots run straight along the [001] direc-

tion, suggesting that the existence of platelike domains perpendicular to the growth direction.

We have taken dark-field images in order to obtain information on the ordered domain morphology. The dark-field images formed using  $\bar{1}/2\ 1/2\ \bar{3}/2, 1/2\ \bar{1}/2\ 1/2$ , and 001 reflections are shown in Figs. 7(a), 7(b), and 7(c), respectively. In Figs. 7(a) and 7(b), the sample was inclined so as to strongly excite the superlattice spot. Note that all photographs were obtained from the identical area in the specimen. Information concerning the  $(\bar{1}11)$  domain is obtained from Fig. 7(a), and that for the  $(1\bar{1}1)$  domain from Fig. 7(b). The microstructures of  $(\bar{1}11)$  domains are entirely different from those of  $(1\bar{1}1)$  ones. In Fig. 7(a), bright regions corresponding to the ordered structure grow from the substrate toward the epilayer surface, and their shape is similar to that of the coarse domain. One can also see that the self-annihilation of APB's occurs particularly at the vicinity of substrate. The features of the structures coincide with those of epitaxial layers obtained through the  $[110]$ -step flow in Fig. 3. More noteworthy is that faint contrasts, which elongate almost parallel to the substrate, are observed inside the coarse domains. The contrast shows that platelike  $(\bar{1}11)$

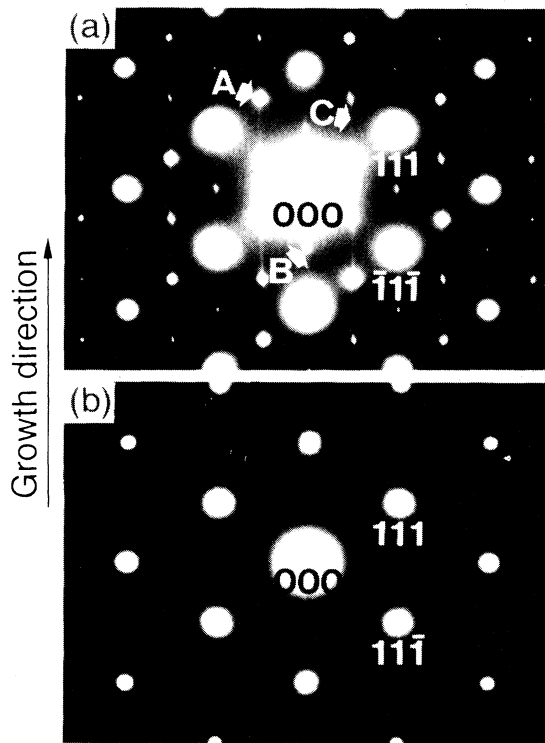


FIG. 6. (a)  $(110)$  and (b)  $(\bar{1}\bar{1}0)$  electron diffraction patterns of a  $\text{Ga}_{1-x}\text{In}_x\text{P}$  layer grown by organometallic vapor phase epitaxy. The misorientation of the GaAs substrate is  $2^\circ$  off in the  $[011]$  direction, thus the substrate includes both  $[110]$  and  $[\bar{1}\bar{1}0]$  surface steps. Besides the fundamental lattice spots of the zincblende structure, there are three characteristic reflections in (a). *A*: CuPt superstructure spot; *B*: the reflection due to double diffraction; and *C*: the diffuse streak. Note that the  $\bar{1}/2\ 1/2\ 1/2$  superlattice spot is stronger than the  $1/2\ \bar{1}/2\ 1/2$  one.

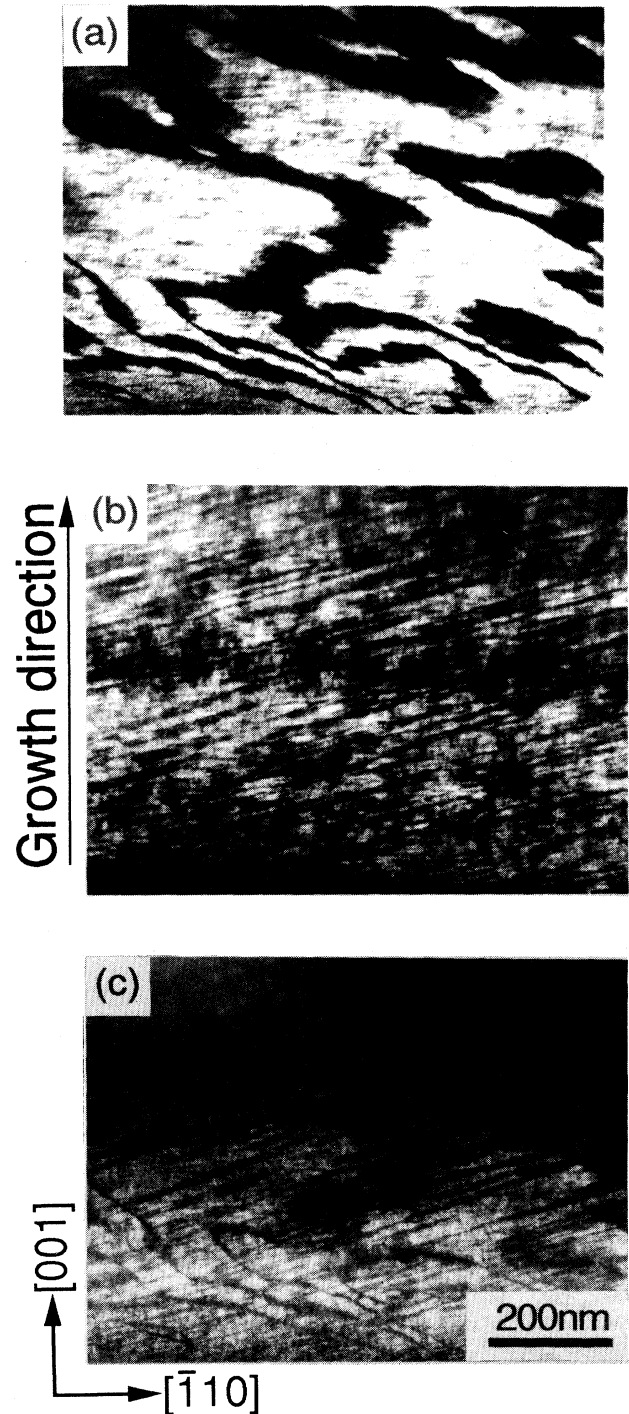


FIG. 7. Dark-field images of the  $\text{Ga}_{1-x}\text{In}_x\text{P}$  layer grown on a  $(001)$  GaAs substrate inclined toward the  $[011]$  direction. Reflections used for forming images are (a)  $\bar{1}/2\ 1/2\ \bar{3}/2$ , (b)  $1/2\ \bar{1}/2\ 1/2$ , and (c) 001 spots, and information about the  $(\bar{1}11)$  and  $(1\bar{1}1)$  CuPt domains is obtained from (a) and (b), respectively. All photographs were taken from the same area in the specimen. The  $(\bar{1}11)$  domains grow from the interface with a substrate up to the top surface of the layer in (a). On the other hand, the  $(1\bar{1}1)$  domains in (b) are platelike in shape, but they slightly incline toward the  $[\bar{1}11]$  direction from  $[\bar{1}10]$ . Note that the faint contrasts exist within the  $(\bar{1}11)$  domain of (a).

domains are also formed by the  $[1\bar{1}0]$ -step flow, and the existence of these domains is thought to cause the diffuse streaks in Fig. 6(a). On the other hand, the coarse domains do not exist in Fig. 7(b). This shows that the  $[110]$  step does not contribute to the formation of the  $(\bar{1}\bar{1}1)$  variant.

The  $(\bar{1}\bar{1}1)$  domains are platelike in shape, but they slightly incline from the interface with a substrate. The appearance of the inclining domain corresponds to the  $1/2\bar{1}/21/2$  reflection in Fig. 6(a), which has a lozenge shape with a larger diagonal tilting from the  $[001]$  direction. The platelike ordered domains tilting slightly from the  $(001)$  plane are often observed by other investigators.<sup>3,24,25</sup> Figure 7(c) suggests that the coarse domains overlap with the fine domains along the  $[110]$  direction. These experimentally observed microstructures are in good agreement with those expected from our simulations, and again confirm the validity of the present treatment for ordering in III-V semiconductor alloys.

#### IV. DISCUSSION

The microstructures of III-V semiconductor alloys depend on the type of surface step. We discuss this phenomenon in terms of the atomic pairwise interactions. First, we consider the formation process of APB's in the case of the  $[110]$ -step flow. In an epilayer grown on a  $(001)$  substrate which is misoriented in the  $[1\bar{1}0]$  direction, APB's are generated from the substrate surface. Figure 8 diagrammatically shows the effect of the interactions on the development of an APB, where only group-III elements are drawn; open and closed circles denote  $A$  and  $B$  atoms, respectively. When a surface step moves toward the APB, like-atom pairs are formed along the  $[1\bar{1}1]$  direction, leaving the atomic arrangements in phase as in Fig. 8(b). When the step is on the APB, the negative intraplane pairwise interactions  $V'_{1h}$  and  $V_{2h}$  re-

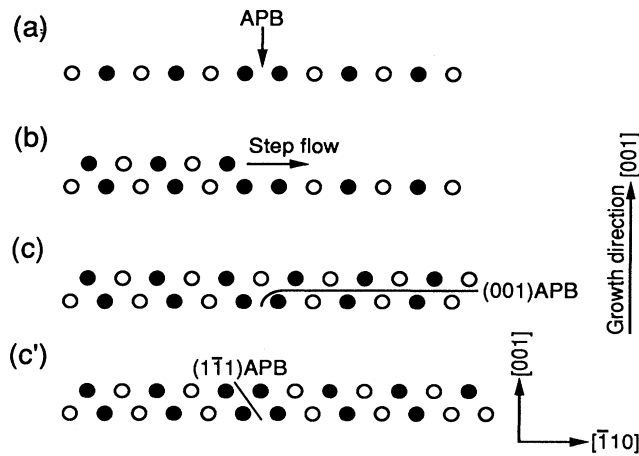


FIG. 8. Formation process of APB parallel to  $(001)$  and  $(\bar{1}\bar{1}1)$ . Only group-III elements are drawn in the diagram. Open circles indicate the  $A$  atom, and closed circles, the  $B$  atom. The relative strength of  $(001)$  intraplane and interplane interactions ( $V_h$  vs  $V_v$ ) determine whether a  $(001)$  or  $(\bar{1}\bar{1}1)$  APB is formed.

sult in a tendency toward the unlike atom, i.e., the  $A$  atom. After the surface step passes over the boundary, a horizontal  $(001)$  APB is left in the crystal [Fig. 8(c)]. Conversely, if the interplane interactions  $V_{1v1}$  and  $V_{1v2}$  are positive, a  $B$  atom is usually attached to the APB, and then the APB is extended along the  $[1\bar{1}1]$  direction [Fig. 8(c')]. Due to the competition of the intraplane and interplane interactions, some parts of an APB become parallel to the  $(\bar{1}\bar{1}1)$  planes and others tend to be pulled in the direction of the step flow, as seen in Fig. 3.

In the case of the  $[1\bar{1}0]$ -step flow, the effective interaction which contributes to the ordering of the  $(001)$  interplanes is  $V_{2v}$  only, as mentioned in Sec. III B. The first-principles calculation<sup>26</sup> has predicted that interactions between second-nearest-neighboring atoms for III-V semiconductor alloys is weak in the bulk state. Correspondingly, the absolute value of  $V_{2v}$  is set to a small value as compared to the growth temperature. Thus thermal fluctuations may easily disturb the ordering along the growth direction, and many plane faults are introduced between the  $(001)$  planes. Conversely, the interactions of the  $(001)$  intraplanes are large enough to develop the ordered structure. Therefore, the CuPt ordering of the  $(001)$  intraplane is faster than that of the  $(001)$

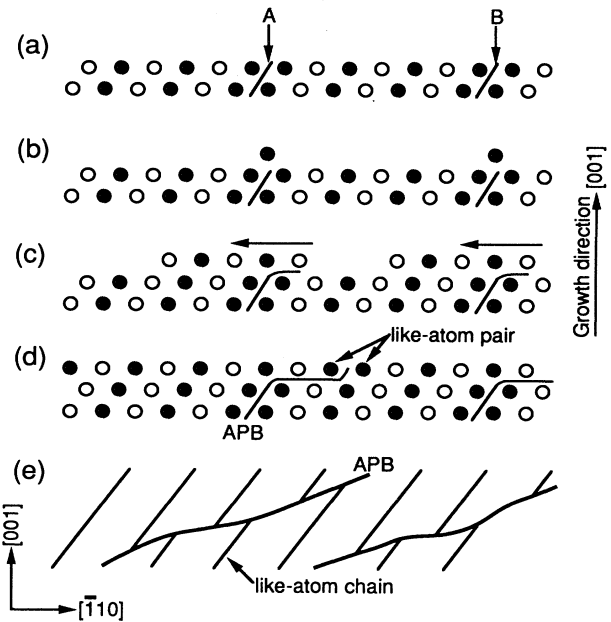


FIG. 9. The formation process of CuPt-type ordered domains tilting from the interface with a substrate. This shows the  $(110)$  cross section of atomic arrangements, and the  $[1\bar{1}0]$  step flows in the  $[110]$  direction. Open and closed circles denote group-III element atoms, and thin lines in (e) denote like-atom chains. (a) Before deposition.  $A$  and  $B$  indicate APB's. (b) A black adatom is adsorbed at  $A$  and  $B$  sites. The adsorbed atoms act as a seed of foregoing deposition. (c) White and black atoms are deposited alternately along  $[1\bar{1}0]$ . The elongation of an ordered phase predominates along the arrow direction. (d) The domains generated from  $A$  and  $B$  sites meet at the right-hand side of the  $A$  site, and another like-atom pair is formed there. (e) The morphology of the ordered domain obtained by repeating procedures (a)–(d).

interplane, and the ordered domains develop to become platelike in the epilayer, as seen in Fig. 5.

According to previous TEM observations,<sup>3,24,25</sup> plate-like ordered domains which tilt from the interface with a (001) substrate are often formed, and the  $(\bar{1}11)$  and  $(1\bar{1}\bar{1})$  domains incline in the  $[\bar{1}\bar{1}\bar{1}]$  and  $[\bar{1}11]$  directions from  $[\bar{1}10]$ , respectively. We consider the formation process of the  $(1\bar{1}\bar{1})$  ordered phase. Figure 9 shows (110) cross sections at the step edge. The step edge is parallel to the paper, and then the direction of the  $[\bar{1}\bar{1}0]$ -step flow is perpendicular to the paper. Black and white circles, which indicate group-III element atoms, are arranged alternately along the  $[\bar{1}\bar{1}0]$  direction, and there are like-atom pairs at APB's, i.e., *A* and *B* sites [Fig. 9(a)]. When an atom which migrates on this layer arrives at the step edge, a black atom is adsorbed at *A* and *B* sites because of positive  $V_{1v1}$  and  $V_{1vr}$  [Fig. 9(b)]. The adsorbed atoms act as a nucleation site of the ordered phase, and the CuPt ordering at the  $[\bar{1}\bar{1}0]$ -step edge occurs from there. The ordering develops easily along the  $[\bar{1}\bar{1}0]$  direction rather than the  $[\bar{1}10]$  one because  $V_{2v}$  is here regarded as negative [Fig. 9(c)], and then a like-atom pair is newly formed at the right-hand side of the *A* site [Fig. 9(d)]. By repeating the above procedure, the  $(1\bar{1}\bar{1})$  domain, which develops from the lower left side to the upper right one, appears in the epilayer [Fig. 9(e)]. The formation process of the slightly tilted  $(\bar{1}11)$  domain can be also explained by the same idea.

## V. CONCLUSION

In the present work, we simulated crystal growth due to the surface step flow in the epitaxy of III-V semiconductor alloys using an Ising-like model for the step flow growth. The findings of this investigation are as follows.

(1) A surface step along the  $[110]$  direction produces ei-

ther of the two CuPt<sub>B</sub>-type variants, depending on the direction of the step motion. The well-developed ordered regions appear from the substrate and extend to the epilayer surface. In the early stages of the growth, the disappearance of APB's occurs due to the self-annihilation process.

(2) After flows of the  $[\bar{1}\bar{1}0]$  step, the  $(\bar{1}11)$  and  $(1\bar{1}\bar{1})$  variants with low degrees of order coexist in the crystal. The ordered domains elongate perpendicularly to the growth direction, and many plane faults, such as APB's and twin boundaries, appear between the (001) planes. The ordering rate in this case is smaller than that in the  $[110]$ -step flow.

(3) When the  $[110]$  and  $[\bar{1}\bar{1}0]$  steps flow in the  $[\bar{1}\bar{1}0]$  and  $[110]$  directions, both of the two CuPt<sub>B</sub> variants appear. The  $(\bar{1}11)$  ordered regions consist of coarse and fine domains. On the other hand, the  $(1\bar{1}\bar{1})$  regions consist of fine domains, suggesting that the  $[110]$  step makes no contribution to the  $(1\bar{1}\bar{1})$  ordering.

(4) The asymmetry of the first-nearest-neighbor interactions of the (001) interlayer at the step edge plays an important role for the morphology of the microstructures and the ordering rate in III-V epilayers obtained by the step flow growth.

## ACKNOWLEDGMENTS

We are grateful to Dr. Suzuki and Dr. Gomyo of the NEC Corporation for kindly providing a specimen of Ga<sub>1-x</sub>In<sub>x</sub>P alloy as well as invaluable discussion. The work was partly supported by Grant-in-Aid for Scientific Research on Priority Areas "Crystal Growth Mechanism in Atomic Scale" Nos. 03243107 and 04227107 and by Nissan Science Foundation (S.M.).

\*Present address: Department of Materials Science and Engineering, Faculty of Engineering, Kyushu University 36, Fukuoka, Fukuoka 812, Japan.

†Present address: Department of Nuclear Engineering, Faculty of Engineering, Kyushu University 36, Fukuoka, Fukuoka 812, Japan.

<sup>1</sup>T. S. Kuan, T. F. Kuech, W. I. Wang, and E. L. Wilkie, Phys. Rev. Lett. **54**, 201 (1985).

<sup>2</sup>A. Gomyo, T. Suzuki, and S. Iijima, Phys. Rev. Lett. **60**, 2645 (1988).

<sup>3</sup>P. Bellon, J. P. Chevalier, E. Augarde, J. P. Andre, and G. P. Martin, J. Appl. Phys. **66**, 2388 (1989).

<sup>4</sup>T. Suzuki and A. Gomyo, J. Cryst. Growth. **111**, 353 (1991).

<sup>5</sup>G. S. Chen, D. H. Jaw, and G. B. Stringfellow, J. Appl. Phys. **69**, 4263 (1991).

<sup>6</sup>D. H. Jaw, G. S. Chen, and G. B. Stringfellow, Appl. Phys. Lett. **59**, 114 (1991).

<sup>7</sup>T. Nishino, J. Cryst. Growth **98**, 44 (1989).

<sup>8</sup>A. Gomyo, T. Suzuki, K. Kobayashi, S. Kawata, and I. Hino, Appl. Phys. Lett. **50**, 673 (1987).

<sup>9</sup>S. R. Kurtz, L. R. Dawson, R. M. Beifeld, D. M. Follstaedt,

and B. L. Doyle, Phys. Rev. B **46**, 1909 (1992).

<sup>10</sup>C. H. Johanson and J. O. Linde, Ann. Phys. (Leipzig) **82**, 449 (1927).

<sup>11</sup>C. H. de Novion and J. P. Landesman, Pure Appl. Chem. **57**, 1391 (1985).

<sup>12</sup>G. P. Srivastava, J. L. Martins, and A. Zunger, Phys. Rev. B **31**, 2561 (1985); **38**, 12 984(E) (1988).

<sup>13</sup>L. G. Ferreira, S.-H. Wei, and A. Zunger, Phys. Rev. B **40**, 3197 (1989).

<sup>14</sup>D. S. Cao, E. H. Reihlen, G. S. Chen, A. W. Kimball, and G. B. Stringfellow, J. Cryst. Growth **109**, 279 (1991).

<sup>15</sup>D. S. Cao, A. W. Kimball, G. S. Chen, K. L. Fry, and G. B. Stringfellow, J. Appl. Phys. **66**, 5384 (1989).

<sup>16</sup>S. Matsumura, N. Kuwano, and K. Oki, Jpn. J. Appl. Phys. **29**, 688 (1990).

<sup>17</sup>S. Matsumura, K. Takano, N. Kuwano, and K. Oki, J. Cryst. Growth **115**, 194 (1991); S. Matsumura, K. Takano, M. Ishimaru, N. Kuwano, and K. Oki (unpublished).

<sup>18</sup>K. Binder and D. W. Heerman, *Monte Carlo Simulation in Statistical Physics, An Introduction* (Springer, Berlin, 1988).

<sup>19</sup>H. Asai, J. Cryst. Growth **80**, 425 (1987).

- <sup>20</sup>I. J. Murgatroyd, A. G. Norman, and G. R. Booker, *J. Appl. Phys.* **67**, 2310 (1990).
- <sup>21</sup>S. Mahajan and B. A. Philips, in *Ordered Intermetallics, Physical Metallurgy and Mechanical Behaviour*, edited by C. T. Liu *et al.* (Kluwer Academic, Dordrecht, The Netherlands, 1992), p. 93.
- <sup>22</sup>S. B. Ogale and A. Madhukar, *Appl. Phys. Lett.* **59**, 1356 (1991); **60**, 2095 (1992).
- <sup>23</sup>R. Osorio, J. E. Bernard, S. Froyen, and A. Zunger, *Phys. Rev. B* **45**, 11 173 (1992).
- <sup>24</sup>C. S. Baxter, W. M. Stobbs, and J. H. Wilkie, *J. Cryst. Growth* **112**, 373 (1991).
- <sup>25</sup>C. S. Baxter, R. F. Broom, and W. M. Stobbs, *Surf. Sci.* **228**, 102 (1990).
- <sup>26</sup>L. G. Ferreira, S.-H. Wei, and A. Zunger, *Phys. Rev. B* **40**, 3197 (1989).

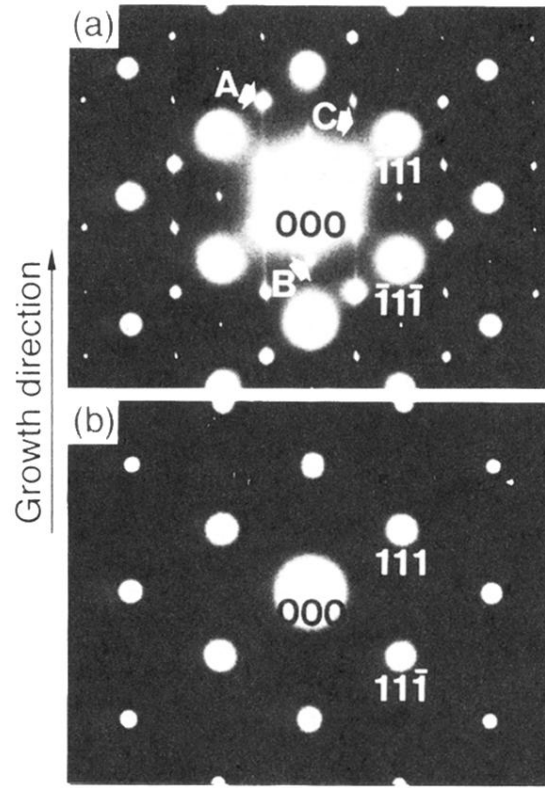


FIG. 6. (a)  $(110)$  and (b)  $(\bar{1}\bar{1}0)$  electron diffraction patterns of a  $\text{Ga}_{1-x}\text{In}_x\text{P}$  layer grown by organometallic vapor phase epitaxy. The misorientation of the GaAs substrate is  $2^\circ$  off in the  $[011]$  direction, thus the substrate includes both  $[110]$  and  $[\bar{1}\bar{1}0]$  surface steps. Besides the fundamental lattice spots of the zincblende structure, there are three characteristic reflections in (a). *A*: CuPt superstructure spot; *B*: the reflection due to double diffraction; and *C*: the diffuse streak. Note that the  $\bar{1}/2\ 1/2\ 1/2$  superlattice spot is stronger than the  $1/2\ \bar{1}/2\ 1/2$  one.

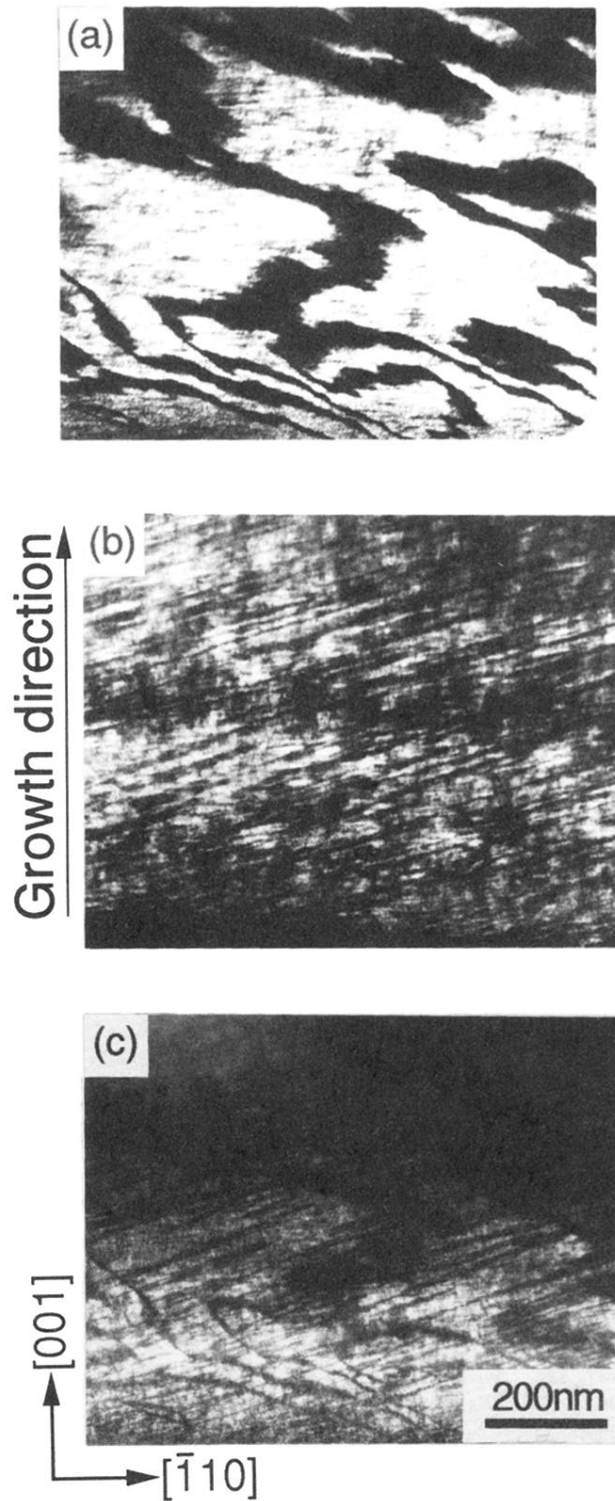


FIG. 7. Dark-field images of the  $\text{Ga}_{1-x}\text{In}_x\text{P}$  layer grown on a (001) GaAs substrate inclined toward the  $[011]$  direction. Reflections used for forming images are (a)  $\bar{1}/2\ 1/2\ \bar{3}/2$ , (b)  $1/2\ \bar{1}/2\ 1/2$ , and (c) 001 spots, and information about the  $(\bar{1}\bar{1}1)$  and  $(1\bar{1}\bar{1})$  CuPt domains is obtained from (a) and (b), respectively. All photographs were taken from the same area in the specimen. The  $(\bar{1}\bar{1}1)$  domains grow from the interface with a substrate up to the top surface of the layer in (a). On the other hand, the  $(1\bar{1}\bar{1})$  domains in (b) are platelike in shape, but they slightly incline toward the  $[\bar{1}\bar{1}1]$  direction from  $[\bar{1}\bar{1}0]$ . Note that the faint contrasts exist within the  $(\bar{1}\bar{1}1)$  domain of (a).